Mathematical Forum ISSN: 0972-9852
Vol.28 (2), 2020

EFFECTS OF BODY FORCES ON WALL SHEAR IN MATHEMATICAL MODELS OF PULSATILE FLOW OF BLOOD THROUGH A CIRCULAR TUBE

ANAND BANSAL[1] and P. CHATURANI[2]
[1]*Department of Mathematics, Government Engineering College, Ajmer- 305 002, India*
[2]*Department of Mathematics (Retd.), IIT Powai, Mumbai – 400 076, India*

Email: [1]dranandbansal@ecajmer.ac.in, [2]pcchaturani@yahoo.com

Received on: 12/06/2020
Accepted on: 20/11/2020

Abstract

Aim of this paper is to investigate the effects of body forces on wall shear in mathematical models of pulsatile blood flow through a circular tube. The wall shear rate has been derived in terms of pressure gradient and body force profiles. The wall shear rates have been calculated for pulsatile flow of blood with and without body forces at twelve different locations of human cardio-vascular system. Experimental body force profile for some real-life situations given by Griffin (1990) have been converted into mathematical forms and presented through Figs. 2 to 5 and corresponding Fourier coefficients have been calculated and given through Tables-1 to 4. A computer program has been developed to compute numerical values of wall shear for different body forces. Wall shear profiles at different locations of a human CVS with body force have been compared with wall shear profiles without body force in four different real-life situations.

Keywords: Body force, wall shear, pulsatile, blood, pressure gradient, transient term, cardio-vascular system (CVS).

2010 AMS Classifications:76Zxx and 76Z05

1. Introduction

In many real-life situations, the human body is subjected to body forces or vibrations, which could be intentional or unintentional. Some of the examples are swinging kids in a cradle for sleep or pleasure, making a subject lie down or vibrating tables as a therapy for heart disease, traveling in road vehicles (car, bus, bicycle, truck, tractor etc.), in water ships, in airplanes and fast body movements in sports activity (playing tennis, bowling in cricket, gymnastics etc.).

Vibrations could be whole body vibrations (like a passenger sitting in a bus/train) or vibrations of a specific part of the body (operation of a jack hammer or lathe machine) or vibrations of body as well as specific part of body (like a driver of a car, bus etc. He gets whole body movement due to the motion of the car, bus, truck etc. and hand vibrations due to holding of steering).

The magnitude, frequency, duration of vibrations and their orientation with respect to the body of the subject play a vital role in the effects of vibrations on the human body [Griffin (1990)]. The information about the vibrations provided by eye does not give a quantitative measure of its severity. It is therefore desirable to analyze the effects of different types of vibrations on different parts of the body.

Such knowledge of body could be useful in the diagnosis and therapeutic treatment of some health problems (joint pain, vision loss and vascular disorders), design of protective pads and machines. It can be also useful in laying down the standards for the body exposure to different types of vibrations.

Aim of the paper is to investigate the effects of body forces on blood flow and wall shear rate.

2. Governing Equations of Motion

In present model, blood is assumed as a viscous incompressible Newtonian fluid flowing through a long rigid tube of radius R placed along z-axis.Due to axial symmetry $\frac{\partial(\,)}{\partial\theta} = 0$, all variables are independent of θ. The variation of velocity along the tube length is considered to be small in comparison to the rate of change of velocity with respect to time and radial distance. The frequency of body force is small so that the wave effects are neglected.

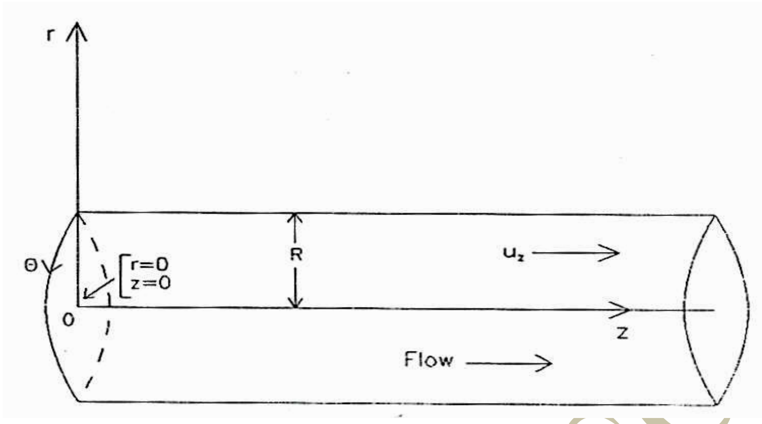

Fig.1: Physical Model of blood flow.

Under these assumptions, the governing equation of motion for the flow of blood in the presence of body force through a rigid tube in a cylindrical polar coordinate system [Sud and Sekhon (1985)] is given by

$$\rho \frac{\partial u_z}{\partial t} = \rho G - \frac{\partial p}{\partial z} + \mu_f \left(\frac{\partial^2 u_z}{\partial r^2} + \frac{1}{r} \frac{\partial u_z}{\partial r} \right), \qquad (1)$$

where ρ *and* μ_f are the density and viscosity of blood, respectively; u_z is the axial component of velocity, G is the body force in axial direction and r is the radial coordinate,

$$-\frac{\partial p}{\partial z} = A_0 + \sum_{n=1}^{\infty} \left[A_n \cos(n\omega_p t) + B_n \sin(n\omega_p t) \right], \qquad t \geq o \qquad (2)$$

p is the pressure which is a function of t and z; z is axial distance, t is time and $\omega_p = 2\pi f_p$, f_p is heart pulse frequency.

The form of body force in terms of Fourier series [Kreyszig (2011)] is given by

$$G = a_0 + \sum_{m=1}^{\infty} \left[a_m \cos(m\omega_b t + \phi_m) + b_m \sin(m\omega_b t + \phi_m) \right], \qquad (3)$$

where $\omega_b = 2\pi f_b$, f_b is its frequency and ϕ_m is its phase difference.

Using equations (3) and (4) into the equation (2), we get

$$\rho \frac{\partial u_z}{\partial t} = \rho a_0 + \rho \sum_{m=1}^{\infty} \left[a_m \cos(m\omega_b t + \phi_m) + b_m \sin(m\omega_b t + \phi_m)\right] + A_0 + \sum_{n=1}^{\infty} \left[A_n \cos(n\omega_p t) + B_n \sin(n\omega_p t)\right] + \mu_f \left(\frac{\partial^2 u_z}{\partial r^2} + \frac{1}{r}\frac{\partial u_z}{\partial r}\right). \tag{4}$$

The initial and boundary conditions [Sud and Sekhon (1985)] are

When t=0; $u_z(r,0) = \dfrac{(R^2 - r^2)\left(A_0 + \sum_{n=1}^{\infty} A_n\right)}{4\mu_f}$,

When t > 0

r =0: $u_z(0,t)$ is finite,

r = R: $u_z(r,t) = 0$, (5)

3. Method of Solution

Applying Laplace transform [Sneddon (1974)] to equation (4) and using ber and bei functions, the expression of the velocity is given by

$$u_z = u_1 + u_2 + u_3 + u_4 + u_5 + \text{Transient term } (u_t), \tag{6}$$

where

$$u_1(r) = (\rho a_0 + A_0)\frac{(R^2 - r^2)}{4\mu_f},$$

$$u_2(t) = \sum_{m=1}^{\infty} \frac{a_m \sin(m\omega_b t + \phi_m) - b_m \cos(m\omega_b t + \phi_m)}{m\omega_b},$$

$$u_3(r,t) = \sum_{m=1}^{\infty} \Big[\big\{\left[a_m \cos(m\omega_b t + \phi_m) + b_m \sin(m\omega_b t + \phi_m)\right]\left[ber_0(\omega_{b1} r) bei_0(\omega_{b1} R) - bei_0(\omega_{b1} r) ber_0(\omega_{b1} R)\right]\left[-a_m \sin(m\omega_b t + \phi_m) + b_m \cos(m\omega_b t + \phi_m)\right] \left[ber_0(\omega_{b1} r) ber_0(\omega_{b1} R) + bei_0(\omega_{b1} r) bei_0(\omega_{b1} R)\right]\big\} / m\omega_b \left\{ber_0^2(\omega_{b1} R) + bei_0^2(\omega_{b1} R)\right\}\Big],$$

$$u_4(t)=\sum_{n=1}^{\infty}\frac{A_n\sin(n\omega_p t)-B_n\cos(n\omega_p t)}{\rho n\omega_p},$$

$$u_5(r,t)=\sum_{n=1}^{\infty}\Big[\{[A_n\cos(n\omega_p t)+B_n\sin(n\omega_p t)][ber_0(\omega_{p1}r)bei_0(\omega_{p1}R)-bei_0(\omega_{p1}r)ber_0(\omega_{p1}R)]$$

$$[-A_n\sin(n\omega_p t)+B_n\cos(n\omega_p t)][ber_0(\omega_{p1}r)ber_0(\omega_{p1}R)+bei_0(\omega_{p1}r)bei_0(\omega_{b1}R)]\}/$$

$$\rho n\omega_p\{ber_0^2(\omega_{p1}R)+bei_0^2(\omega_{p1}R)\}\Big],$$

$$\text{Transient term }(u_t)=2\sum_{k=1}^{\infty}\frac{e^{-\eta\lambda_k^2 t}}{\rho\eta\lambda_k^3 J_1(\lambda_k)}J_0\left(\frac{r}{R}\lambda_k\right)\Bigg\{\left(-\rho a_0+\sum_{n=1}^{\infty}A_n\right)-$$

$$\rho\sum_{m=1}^{\infty}\frac{[a_m(\eta^2\lambda_k^4\cos\phi_m+m\omega_b\eta\lambda_k^2\sin\phi_m)+b_m(-m\omega_b\eta\lambda_k^2\cos\phi_m+\eta^2\lambda_k^4\sin\phi_m)]}{(\eta^2\lambda_k^4+m^2\omega_b^2)}-$$

$$\sum_{n=1}^{\infty}\left[\frac{\eta^2\lambda_k^4 A_n-n\omega_p\eta\lambda_k^2 B_n}{(\eta^2\lambda_k^4+n^2\omega_b^2)}\right]\Bigg\}, \quad (7)$$

4. Wall Shear

The wall shear τ_ω is given by

$$\tau_\omega=\mu_f\left.\frac{\partial u_z(r,t)}{\partial r}\right|_{r=R}. \quad (8)$$

Hence, the expression of wall shear τ_ω is obtained of the form given below

$$
\begin{aligned}
\tau_{\omega} &= -\frac{1}{2}(\rho a_0 + A_0)R + \\
&\sqrt{\frac{\mu_f \rho}{2\omega_b}} \sum_{m=1}^{\infty} \Big[\Big\{\big[a_m \cos(m\omega_b t + \phi_m) + b_m \sin(m\omega_b t + \phi_m)\big]\big[\{ber_1(\omega_{b1}R) + bei_1(\omega_{b1}R)\} bei_0(\omega_{b1}R) - \\
&\quad \{bei_1(\omega_{b1}R) - ber_1(\omega_{b1}R)\} ber_0(\omega_{b1}R)\ \big] + \big[-a_m \sin(m\omega_b t + \phi_m) + b_m \cos(m\omega_b t + \phi_m)\big] \\
&\quad \big[\{ber_1(\omega_{b1}R) + bei_1(\omega_{b1}R)\} ber_0(\omega_{b1}R) + \{bei_1(\omega_{b1}R) - ber_1(\omega_{b1}R)\} bei_0(\omega_{b1}R)\big]\Big\} / \\
&\quad \sqrt{m}\,\{ber_0^2(\omega_{b1}R) + bei_0^2(\omega_{b1}R)\}\ \Big] + \sqrt{\frac{\mu_f}{2\omega_p \rho}} \sum_{n=1}^{\infty} \Big[\Big\{\big[A_n \cos(n\omega_p t) + B_n \sin(n\omega_p t)\big] \\
&\quad \big[\{ber_1(\omega_{p1}R) + bei_1(\omega_{p1}R)\} bei_0(\omega_{p1}R) - \{bei_1(\omega_{p1}R) - ber_1(\omega_{p1}R)\} ber_0(\omega_{p1}R)\big] \\
&\quad + \big[-A_n \sin(n\omega_p t) + B_n \cos(n\omega_p t)\big]\ \big[\{ber_1(\omega_{p1}R) + bei_1(\omega_{p1}R)\} ber_0(\omega_{p1}R) + \\
&\quad \{bei_1(\omega_{p1}R) - ber_1(\omega_{p1}R)\} bei_0(\omega_{p1}R)\big]\Big\} / \sqrt{n}\,\{ber_0^2(\omega_{p1}R) + bei_0^2(\omega_{p1}R)\}\Big]. \qquad (9)
\end{aligned}
$$

5. Body Force Profiles

Griffin (1990) presented some experimental body force profiles for some real-life situations as given below

(i) Body force profile for vertical vibrations on the seat of ship, during sea travel (f_b = 0.2 Hz),

(ii) Body force profile for vertical head vibrations during gentle jogging(f_b = 2.24 Hz),

(iii) Body force profile for vertical vibrations on the seat of a tractor (f_b = 3.2 Hz),

(iv) Body force profile for hand vibrations while operating chipping tool(f_b = 51.2 Hz).

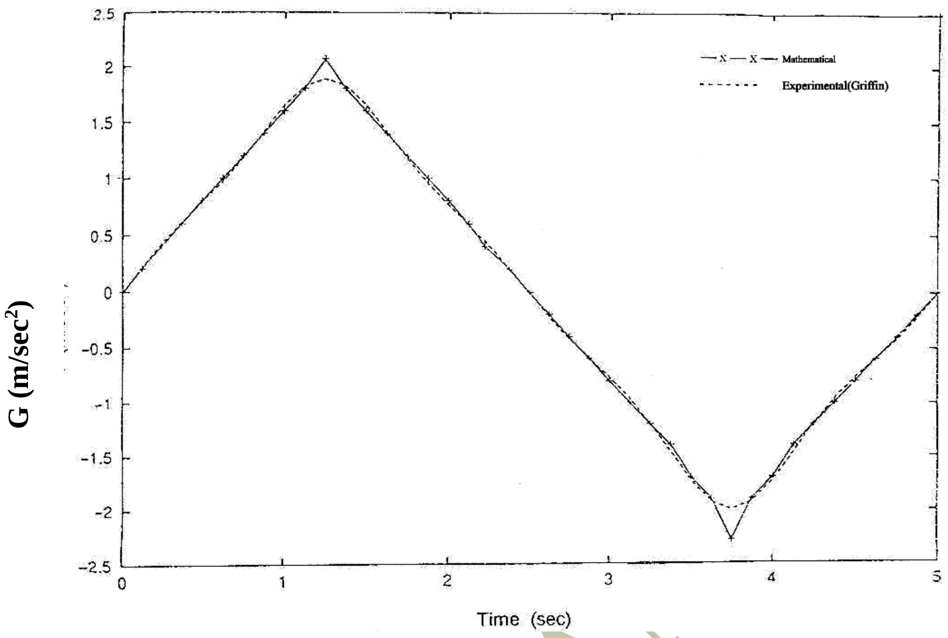

Fig.2: A comparison of experimental and mathematical forms of body force profile: vertical vibrations on the seat of ship, during sea travel [Griffin (1990)], f_b =0.2 Hz.

Table-1: Values of Fourier coefficients for body force profile (in m sec^{-2})

a_0	n	a_n	b_n
-16.27	1	1.42	1732.53
	2	24.20	5.78
	3	0.96	-221.41
	4	-18.98	3.39
	5	-3.78	87.52

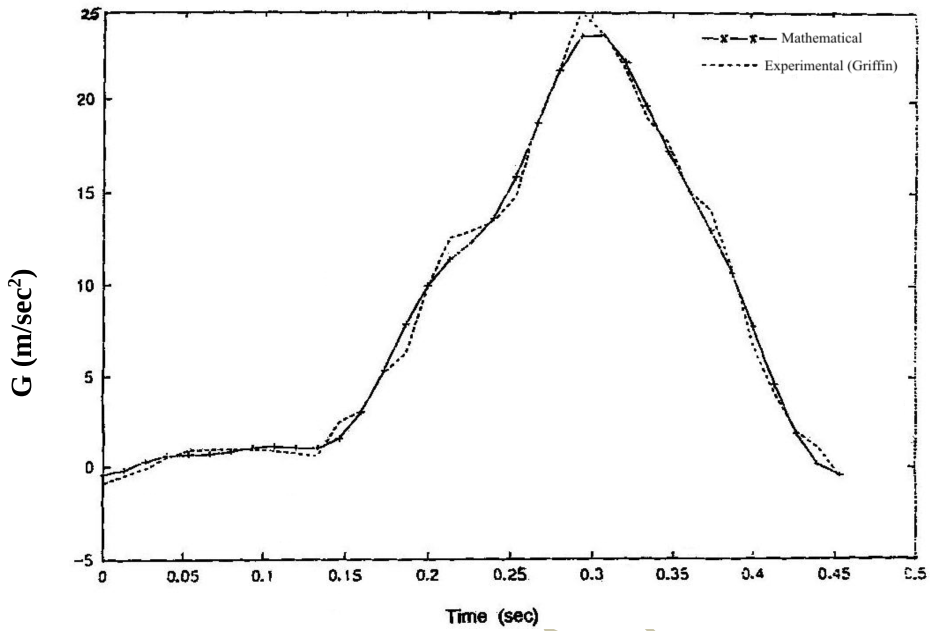

Fig.3: A comparison of experimental and mathematical forms of body force profile: vertical head vibrations during gentle jogging [Griffin (1990)], f_b =2.24 Hz.

Table-2: Values of Fourier coefficients for body force profile (in m sec^{-2})

a_0	n	a_n	b_n
8893.26	1	-6649.85	-9289.20
	2	-2007.97	2518.24
	3	-21.35	665.77
	4	-616.51	-558.15
	5	-41.25	833.75

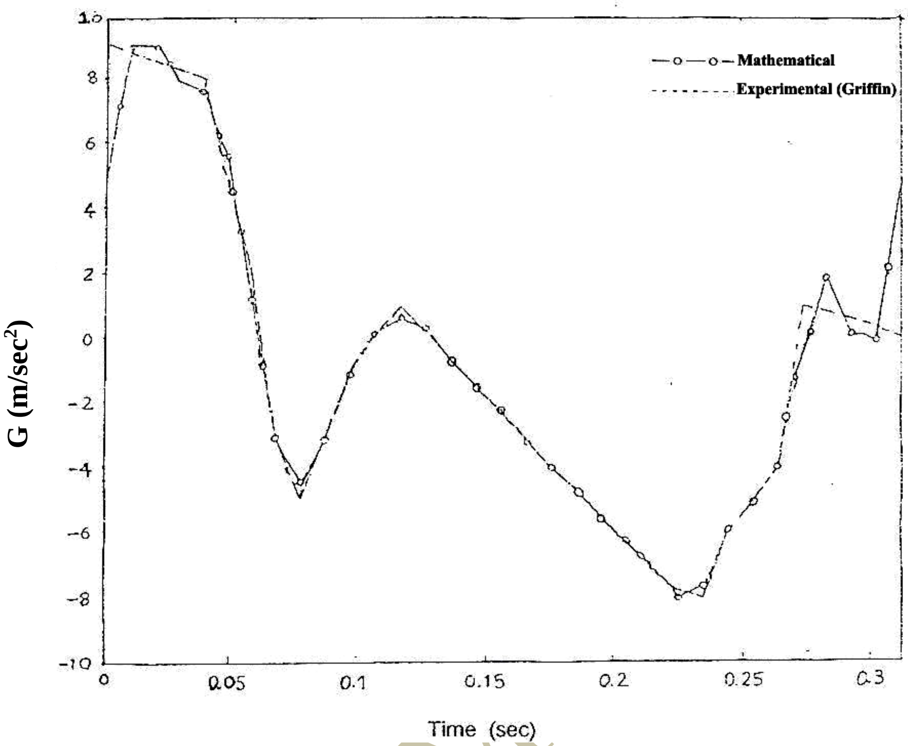

Fig.4: A comparison of experimental and mathematical forms of body force profile: vertical vibrations on the seat of a tractor [Griffin (1990)], f_b =3.2 Hz.

Table-3: Values of Fourier coefficients for body force profile (in m sec^{-2})

a_0	n	a_n	b_n
-986.24	1	3898.81	3819.84
	2	3456.87	774.96
	3	-36.29	1755.82
	4	-1552.98	676.75
	5	-389.68	-45.24
	6	213.25	369.25
	7	21.74	742.01
	8	11.73	755.55
	9	120.57	401.36
	10	175.94	64.22

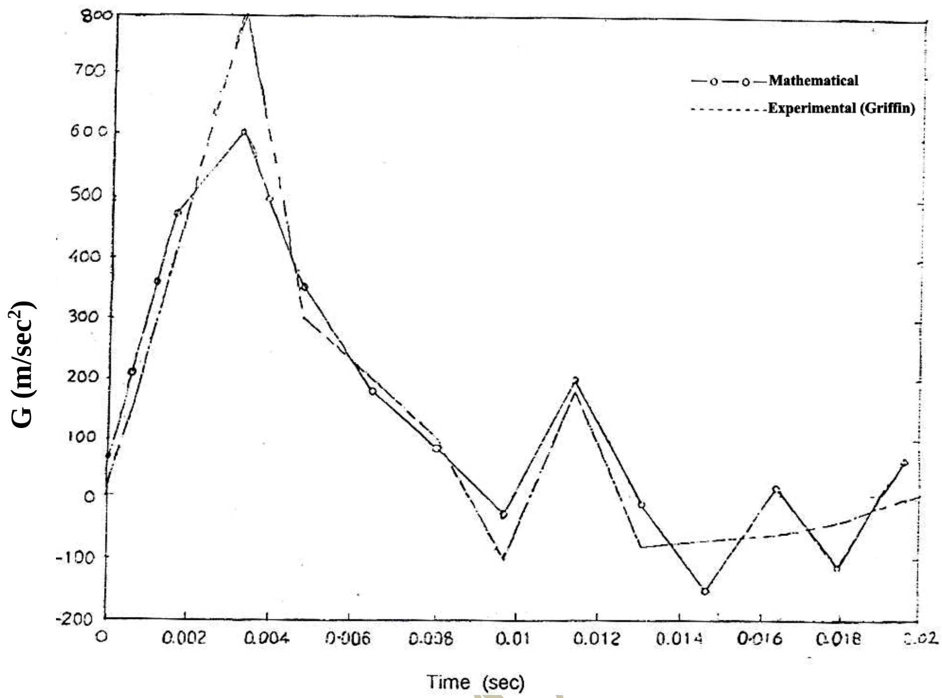

Fig.5: Experimental and Mathematical forms of body force profile: hand vibrations while operating chipping tool [Griffin (1990)], f_b =51.2 Hz.

Table-4: Values of Fourier coefficients for body force profile (in m sec^{-2})

a_0	n	a_n	b_n
145.39	1	66.50	241.13
	2	-38.01	167.57
	3	-64.15	-2.16
	4	-84.95	47.77
	5	40.09	8.57

(i) Effects of body force (vertical vibrations on the seat of ship) on wall shearprofiles.

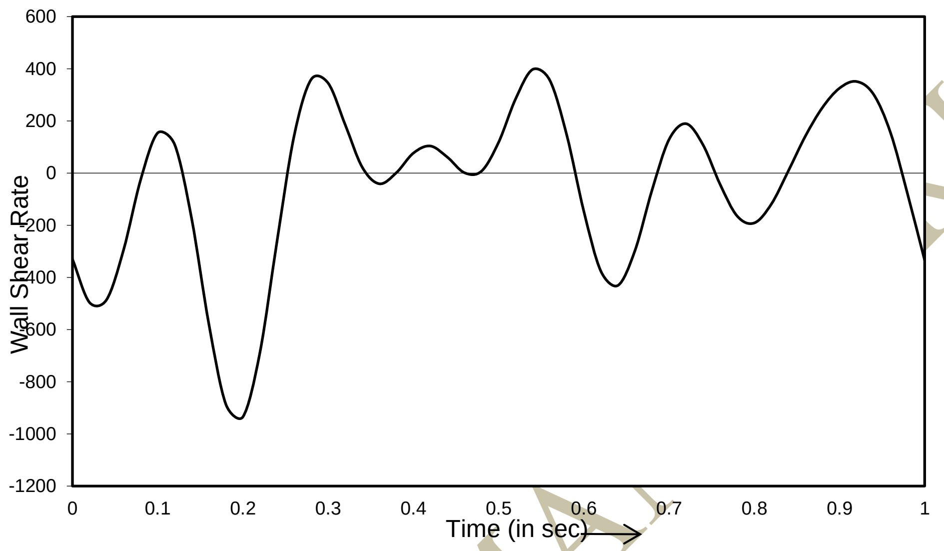

Fig.6: Wall shear profile for superficial femoral artery [Hwang and Normann (1977)] without body force.

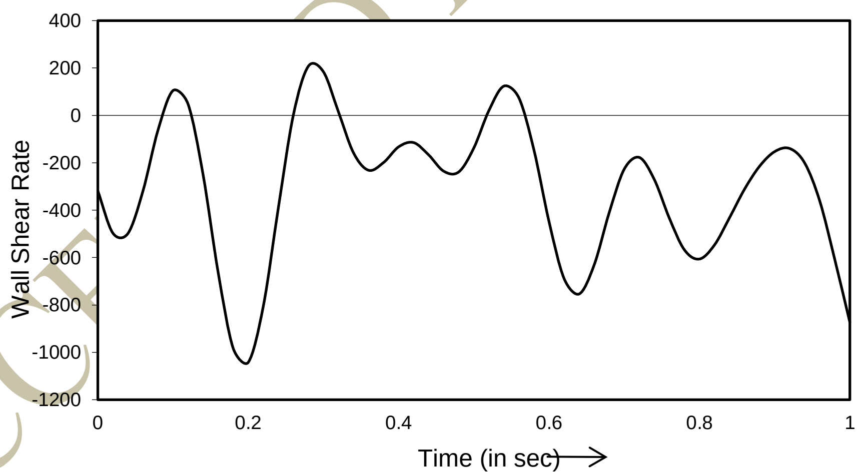

Fig.7: Wall shear profile for superficial femoral artery [Hwang and Normann (1977)] with body force (traveling in a ship).

It is seen from Figs. 6 and 7 that wall shear assumes non-periodic, positive as well as negative values for body force at superficial femoral artery.

(ii) Effects of body force (vertical head vibrations during gentle jogging) on wall shear.

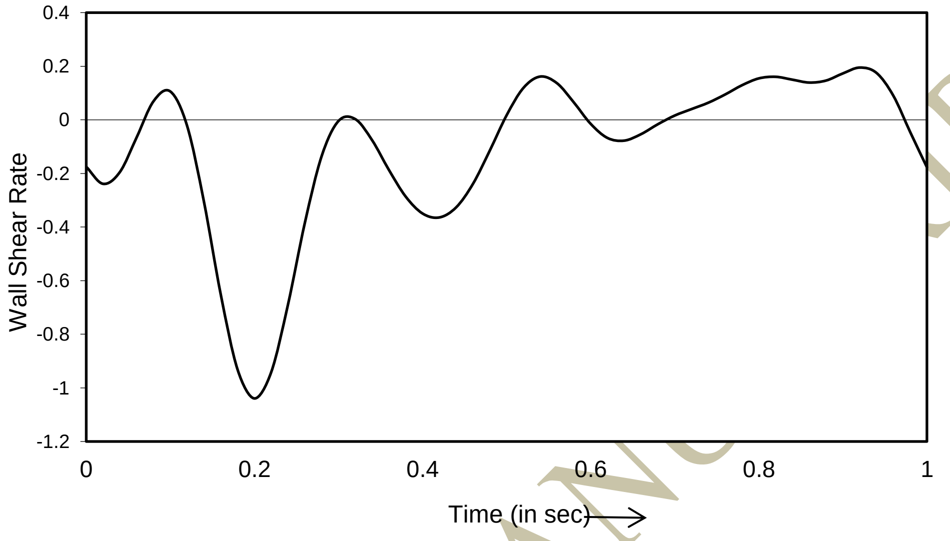

Fig.8: Wall shear profile for common iliac artery [Hwang and Normann (1977)] without body force.

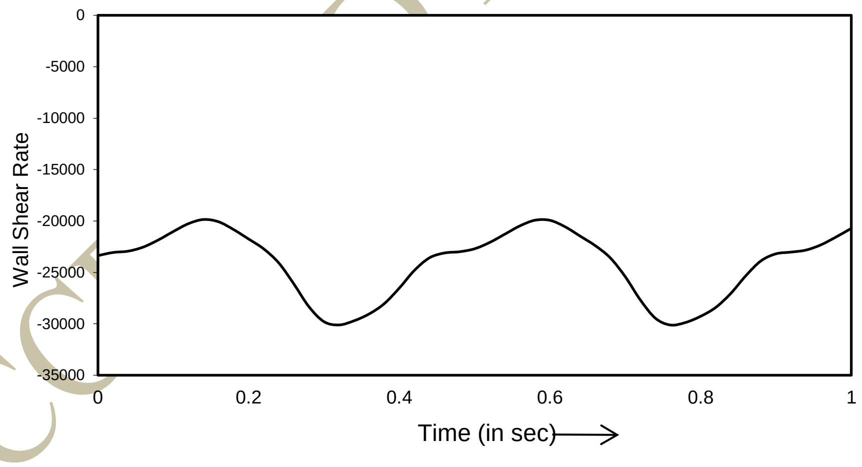

Fig.9: Wall shear profile for common iliac artery [Hwang and Normann (1977)] with body force (gentle jogging).

It is observed from Figs. 8 and 9 that wall shear is assuming periodic values at common iliac artery.

(iii) Effects of body force (vertical vibrations on the seat of a tractor) on wall shear.

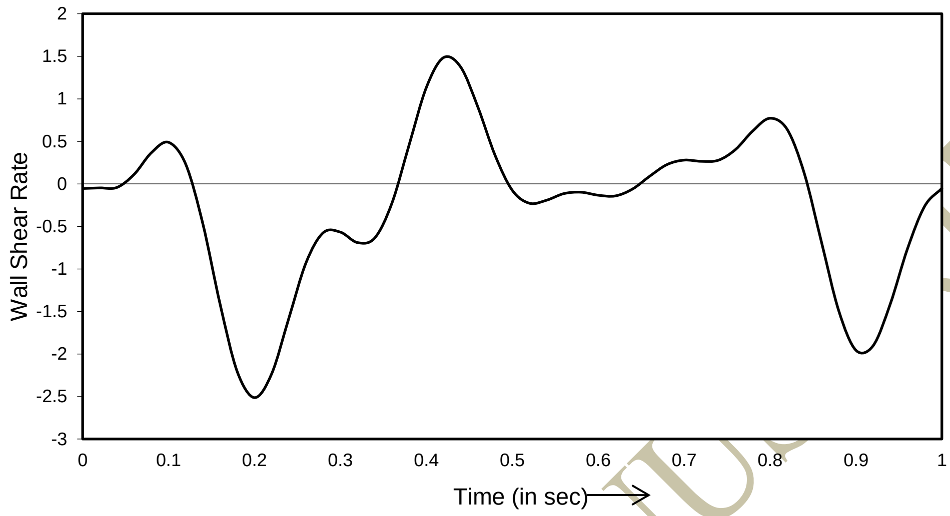

Fig.10: Wall shear profile for axillary artery [Hwang and Normann (1977)] without body force.

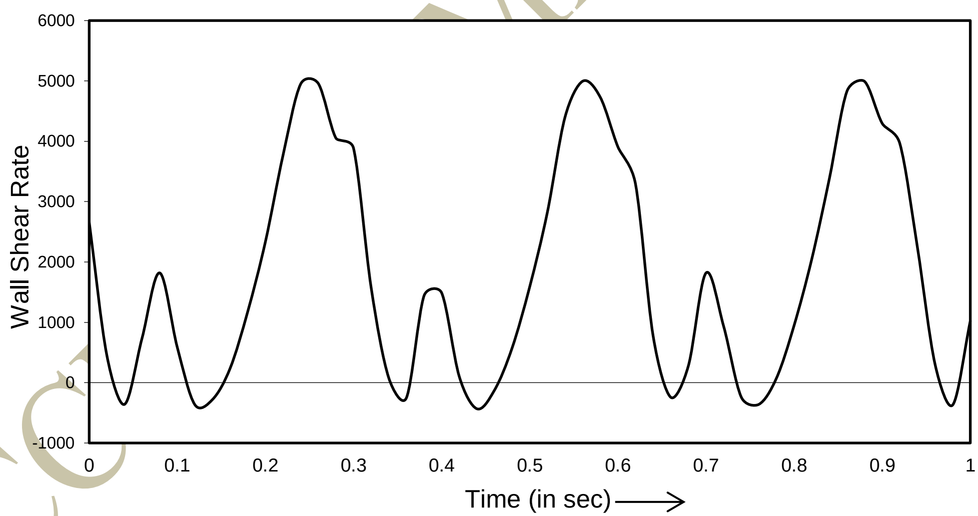

Fig.11: Wall shear profile for axillary artery [Hwang and Normann (1977)] with body force (sitting in a tractor).

It is observed from Figs. 10 and 11 that wall shear has periodic positive with slightly negative values at some points at axillary artery.

(iv) Effects of body force (hand vibrations while operating chipping tool) on wall shear.

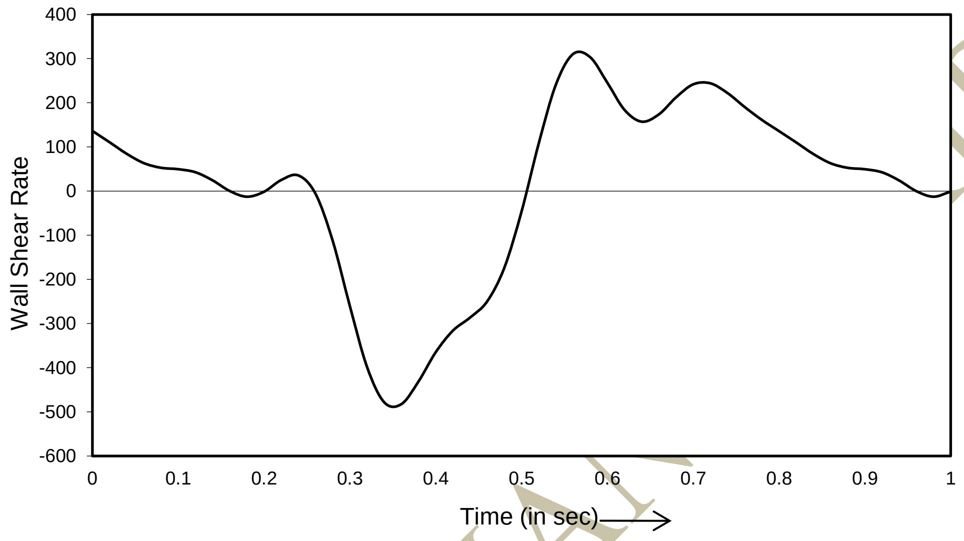

Fig.12: Wall shear profile for pulmonary artery [Milnor (1989)] without body force.

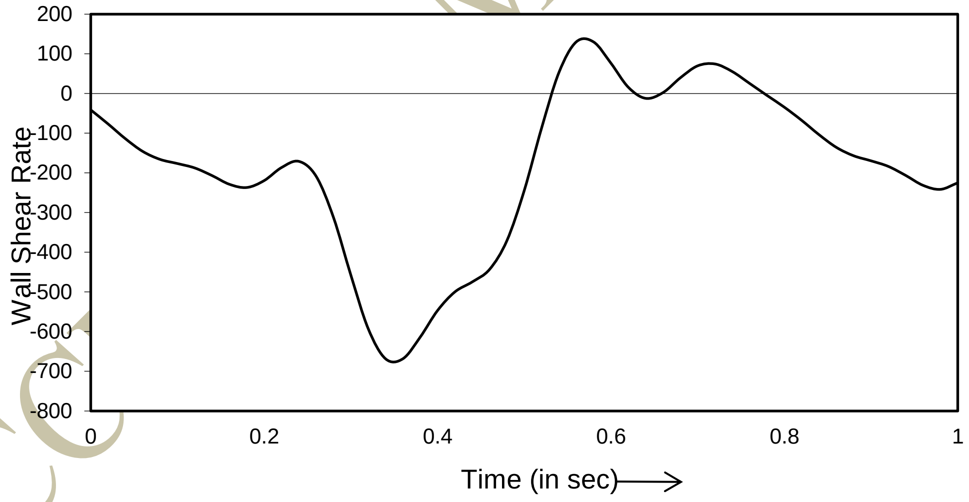

Fig.13: Wall shear profile for pulmonary artery [Milnor (1989)] with body force (operating chipping tool).

Figs. 12 and 13 depict that wall shear takes both positive and negative values withperiod 0.82 sec for pulmonary artery.

6. Results and Discussion

In the literature [Womersley (1955), Lightfoot (1974), Sud and Sekhon (1985, 1986), Chaturani and Palanisamy (1991), Mishra (2010), Bessonov (2016) etc.], ideal form of inputs (pressure gradient and body force) has been used. But in this paper, better pressure gradient [Bansal (2005)] and body force profiles [Griffin (1990)] are used.

Sud and Sekhon (1985) obtained exact analytic solution for velocity in terms of Bessel functions of the first kind with a complex argument. They did not derive expression of wall shear from exact solutions and obtained approximate solutions. In the present work, exact analytic expression for wall shear is obtained in real form by using ber and bei functions.

Experimental body forces given by Griffin (1990) are converted into mathematical forms and presented through Figures. Fourier coefficients of body force profiles are given through Tables. The expression of wall shear is obtained for pulsatile flow with and without body force. Wall shear profiles are obtained at different locations in human CVS by using four different body forces.

7. Conclusions

Analytic solutions for velocity and wall shear have been obtained by using Laplace transform technique and Bessel functions theory. Experimental body forces given by Griffin (1990) have been converted into mathematical formsand presented through Figs. 2 to 5 and corresponding Fourier coefficients have been calculated and given through Tables-1 to 4.

Thus, obtained mathematical form of body forces can be readily used as input in mathematical models to study the effect of body forces on pulsatile flow of blood for human beings. A computer program in C++ Language is developed to compute numerical values of wall shear with different body forces and without body forces.

Effects of body forces on wall shear profiles in in human CVS are presented through figures. Wall shear profiles with four different body forces are compared with wall shear profile without body force. For very low frequency (f_b = 0.2 Hz), of body force, wall shear rate appears to be decrease rapidly.

The time period of wall shear without body forces is about one second, while the time period of wall shear with body forces depends upon frequencies of body forces. For different body forces, different time periods of wall shear profiles are observed. So, body force can be used to reduce the time period of wall shear. Body force can also be used to increase the frequency of wall shear, which may cause wall muscle fatigue.

Hence, it is noticed that body force controls the form of the wall shear profiles. Body force alters the negative velocity duration. This in turn gives a control on back flow regions, their duration and size. The time and size of back flow regions play an important role in many arterial diseases [Young (1979)].

References

[1] Bansal, A.(2005), A study of Mathematical models of Blood flow in Bio-fluid Dynamics, Ph.D. Thesis, University of Rajasthan, Jaipur, 2005.

[2] Bessonov, N., Sequeira, A., Simakov, S., Vassilevskii, Yu. and Volpert, V. (2016), Methods of Blood Flow Modelling, Math. Model. Nat. Phenom., 11(1),1-25.

[3] Chaturani, P. and Palanisamy, V. (1990), Casson fluid model for pulsatile flow of blood under periodic body acceleration, Biorheology, 27, 619-630.

[4] Chaturani, P. and Palanisamy, V. (1990), Pulsatile flow of power law fluid model for blood flow under periodic body acceleration, Biorheology, 27, 747-758.

[5] Chaturani, P. and Palanisamy, V. (1991), Pulsatile flow of blood with periodic body acceleration, Int. J. Engg. Sci., 29(1), 113-121.

[6] Griffin, M.J. (1990), Handbook of Human Vibration, Academic Press Ltd., London, 1990.

[7] Hwang, N.H.C. and Normann, N.A.E. (1977), Cardiovascular Flow Dynamics and Measurements, University Park Press, Baltimore, 1977.

[8] Kreyszig, E. (2011), Advanced Engineering Mathematics, 10th Ed., John Wiley and Sons, Inc., New York, 2011.

[9] Kumar, S. (2009), A mathematical model for Newtonian and non-Newtonian flow through tapered tube, Indian Journal of Biomechanics: Special Issue (NCBM), 191-195.

[10] Lightfoot, E.N.(1974), Transport Phenomena and Living Systems, John Wiley and Sons Inc., New York, 1974.

[11] Milnor, W.R. (1989), Hemodynamics, Williams and Wilkins, London, 1989.

[12] Mishra, B.K., Pradhan, P. and Panda, T.C. (2010), Effect of shear stress, resistance and flow rate across mild stenosis on Blood Flow through Blood Vessels, The Cardiology, 5(1), 4-11.

[13] Sneddon, I.N. (1974), The use of Integral Transforms, McGraw Hill, New York, 1974.

[14] Sud, V.K. and Sekhon, G.S. (1985), Analysis of blood flow under periodic time dependent body acceleration, Med. Biol. Engg. and Compt., 23, 69-73.

[15] Sud, V.K. and Sekhon, G.S. (1985), Arterial flow under periodic body acceleration, Bull. Math. Biol., 47(1), 35-52.

[16] Sud, V.K. and Sekhon, G.S. (1986), Analysis of blood flow through a model of human arterial system under periodic time dependent body acceleration, J. Biomech., 19, 929-941.

[17] Womersley, J.R. (1955), Method for the calculation of velocity, rate of flow and viscous drag in arteries when the pressure gradient is known, J. Physiol.,127, 553-563.

[18] Young, D.F.(1979), Fluid Mechanics of Arterial Stenosis, Trans. ASME. J. Biomech. Engg.,101, 157.